

Motor- and Tail-Dependent Targeting of Dynein to Microtubule Plus Ends and the Cell Cortex

Steven M. Markus,¹ Jesse J. Punch,¹ and Wei-Lih Lee^{1,*}

¹Biology Department
University of Massachusetts at Amherst
221 Morrill South
611 North Pleasant Street
Amherst, MA 01003
USA

Summary

Background: Cytoplasmic dynein mediates spindle positioning in budding yeast by powering sliding of microtubules along the cell cortex. Although previous studies have demonstrated cortical and plus-end targeting of dynein heavy chain (Dyn1/HC), the regulation of its recruitment to these sites remains elusive.

Results: Here we show that separate domains of Dyn1/HC confer differential localization to the dynein complex. The N-terminal tail domain targets Dyn1/HC to cortical Num1 receptor sites, whereas the C-terminal motor domain targets Dyn1/HC to microtubule plus ends in a Bik1/CLIP-170- and Pac1/LIS1-dependent manner. Surprisingly, the isolated motor domain blocks plus-end targeting of Dyn1/HC, leading to a dominant-negative effect on dynein function. Overexpression of Pac1/LIS1, but not Bik1/CLIP-170, rescues the dominant negativity by restoring Dyn1/HC to plus ends. In contrast, the isolated tail domain has no inhibitory effect on Dyn1/HC targeting and function. However, cortical targeting of the tail construct is more robust than full-length Dyn1/HC and occurs independently of Bik1/CLIP-170 or Pac1/LIS1.

Conclusions: Our results suggest that the cortical association domain is normally masked in the full-length dynein molecule. We propose that targeting of dynein to plus ends unmasks the tail, priming the motor for off-loading to cortical Num1 sites.

Introduction

Cytoplasmic dynein is a minus-end-directed microtubule motor that participates in a variety of motile activities during mitosis, including centrosome separation [1], nuclear envelope breakdown [2], chromosome capture and congression [3], mitotic spindle assembly [4], spindle pole organization [5], spindle alignment [6, 7], and spindle checkpoint inactivation [8, 9]. The heavy chain of dynein consists of a ring of six AAA (ATPases associated with cellular activities) units [10, 11], which form the motor domain that powers movement along microtubules, and the tail domain, which binds accessory chains and adaptor molecules that attach the motor to diverse cellular cargoes [12–15]. To perform all of its tasks during mitosis, the cargo-binding tail domain must specify targeting of dynein to different subcellular sites in a spatially and temporally defined manner. Although various studies [2, 6–9, 16–20] have implicated the tail domain as playing a pivotal role, the mechanism by which this domain regulates dynein

localization is not known. Additionally, whether the motor domain has any role in dynein targeting is not known.

In this study, we examined the roles of the tail and motor domains in dynein localization and function in the budding yeast *S. cerevisiae*. We found that these two domains play distinct but complementary roles in mediating the spatial targeting of dynein. We identified a novel role for the motor domain in dynein targeting and revealed a new regulatory step mediated by the tail domain in the off-loading model for dynein function in spindle positioning.

Results

The Tail Domain Targets Dynein to Cortical Num1 Sites

Dyn1/HC localizes as foci at the spindle pole body (SPB), microtubule plus ends, and the cell cortex [17, 21–24]. We set out to test the hypothesis that the tail domain of Dyn1/HC is responsible for its targeting. We altered the *DYN1* locus to express only the tail domain (amino acids 1–1363) fused with 3GFP under its native promoter. Haploid cells carrying *TAIL-3GFP* as their sole source of dynein exhibited cortical foci at all cell-cycle stages (Figure 1B). Notably, these cells contained no SPB or plus-end-associated foci. Cortical tail-3GFP foci were stationary (Movie S1 available online) and were found at the mother and daughter cortex (Figure 1B), as previously described for Dyn1/HC-3GFP cortical foci [17]. In some cases (<10% of cells), we observed cytoplasmic tail-3GFP foci, which were not associated with microtubules and may represent tail-3GFP aggregates. *TAIL-3GFP* and *DYN1/HC-3GFP* strains exhibited similar levels of increase in the percentage of cortical-foci-containing cells as they entered preanaphase (Figure 2A; 2.2-fold for *DYN1/HC-3GFP* and 1.7-fold for *TAIL-3GFP*), suggesting that the temporal regulation of cortical association for tail-3GFP is similar to Dyn1/HC-3GFP. However, the likelihood of finding a cortical focus was significantly higher in the *TAIL-3GFP* strain than in the *DYN1/HC-3GFP* strain. Whereas cortical Dyn1/HC-3GFP foci were observed in 17.9% ± 1.9% (n = 431) of cells, cortical tail-3GFP foci were observed in 65.1% ± 2.0% (n = 581) of cells. Additionally, full 3D stacks of confocal sections showed that there are 7.8 ± 3.3 (n = 87) cortical tail-3GFP foci per cell (Movies S2 and S3), compared to 3.8 cortical foci per cell for Dyn1/HC-3GFP [17]. This large discrepancy in cortical targeting between tail-3GFP and Dyn1/HC-3GFP could not be attributed to an affinity of Dyn1/HC-3GFP for microtubules (Figure S1F). Instead, the discrepancy indicates that the isolated tail domain is lacking a regulatory component for cortical association compared to Dyn1/HC. It suggests a role for the motor domain in masking the tail domain from cortical association in the context of the full-length molecule.

We previously proposed a dynein off-loading model in which Dyn1/HC is delivered by microtubule plus ends to the cortex, where Dyn1/HC becomes anchored at cortical Num1 sites in order to generate forces for pulling the spindle [22, 24]. We asked whether tail-3GFP localizes to Num1 sites, as would be expected if the tail domain is responsible for anchoring dynein to Num1. We observed that the majority of tail-3GFP foci colocalized with a cortical Num1-mCherry focus

*Correspondence: wlee@bio.umass.edu

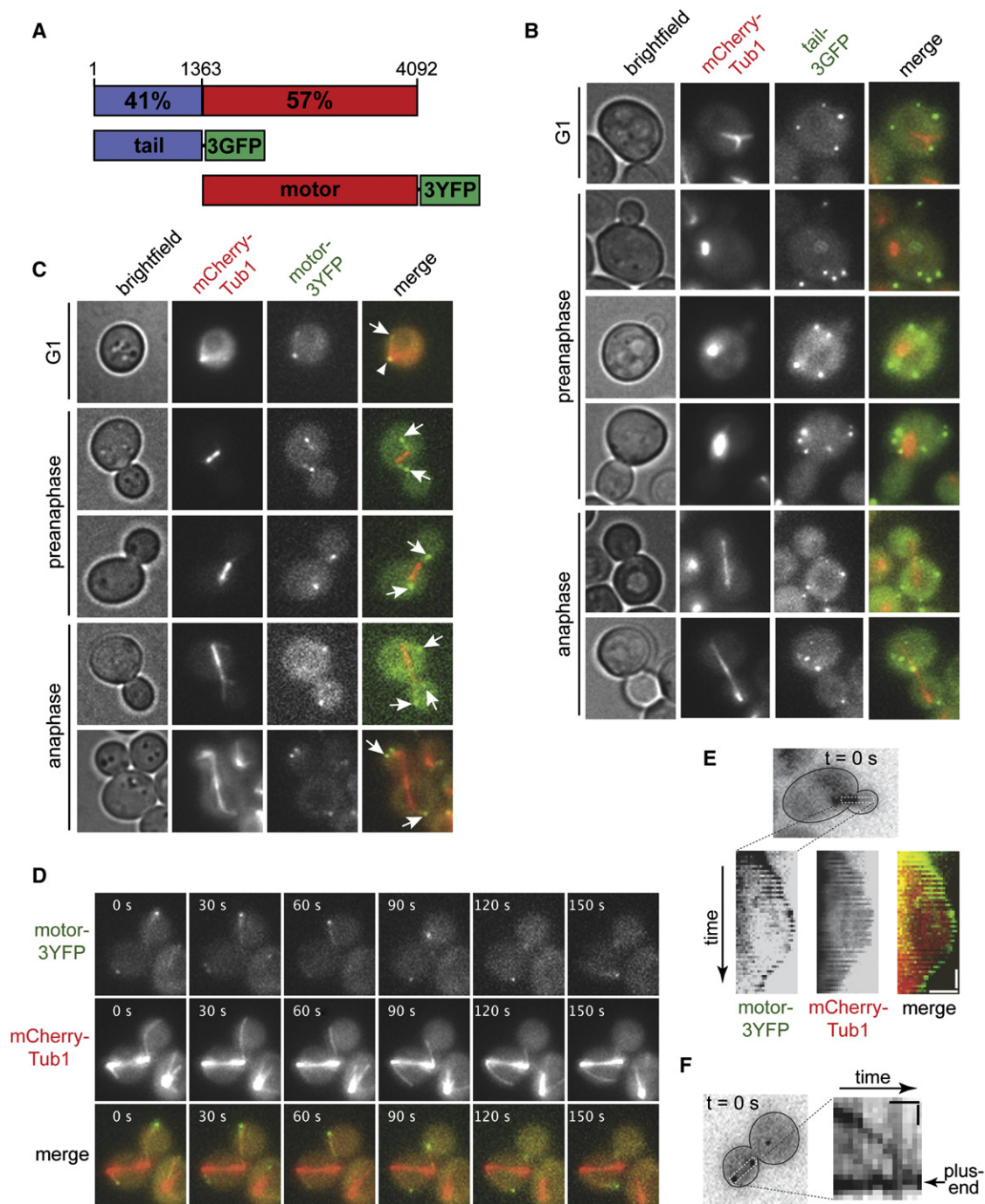


Figure 1. Isolated Dynein Tail and Motor Domains Localize to Distinct Subcellular Sites

(A) Schematic representation of Dyn1/HC constructs used in this study. Percent similarity to corresponding rat DYNC1H1 domain is indicated (see [Figure S1A](#)). Numbering indicates amino acid residues.

(B) Tail-3GFP localizes as stationary foci at the cell cortex throughout the cell cycle (see [Movie S1](#)).

(C) Motor-3YFP localizes to SPB and microtubule plus ends throughout the cell cycle.

(B and C) Arrows indicate plus-end foci; arrowhead indicates SPB focus. Brightfield and maximum intensity projection of wide-field fluorescence images of cells expressing either (B) tail-3GFP or (C) motor-3YFP under the control of the endogenous *DYN1* promoter, and mCherry-Tub1 under the control of the *MET3* promoter. Merged image on the right depicts tail-3GFP or motor-3YFP in green and mCherry-Tub1 in red.

(D) Representative movie frames of motor-3YFP and mCherry-Tub1 depicting motor-3YFP at shrinking and growing microtubules in the same cell. Each image is a maximum intensity projection of a 2 μ m Z-stack of wide-field images. The time elapsed in seconds is indicated (see [Movie S4](#)).

(E) Kymograph depicting motor-3YFP tip-tracking on a polymerizing and depolymerizing cytoplasmic microtubule (see [Movie S5](#)). Vertical bar represents 20 s; horizontal bar represents 2 μ m.

(F) Kymograph depicting directional movement of motor-3YFP along a cytoplasmic microtubule toward the plus end (see [Movie S6](#)). Vertical bar represents 10 s; horizontal bar represents 1 μ m. Plus-end-associated motor-3YFP was used as a reference point to crop images, allowing the plus end to appear stationary with respect to the focus migrating toward the plus end.

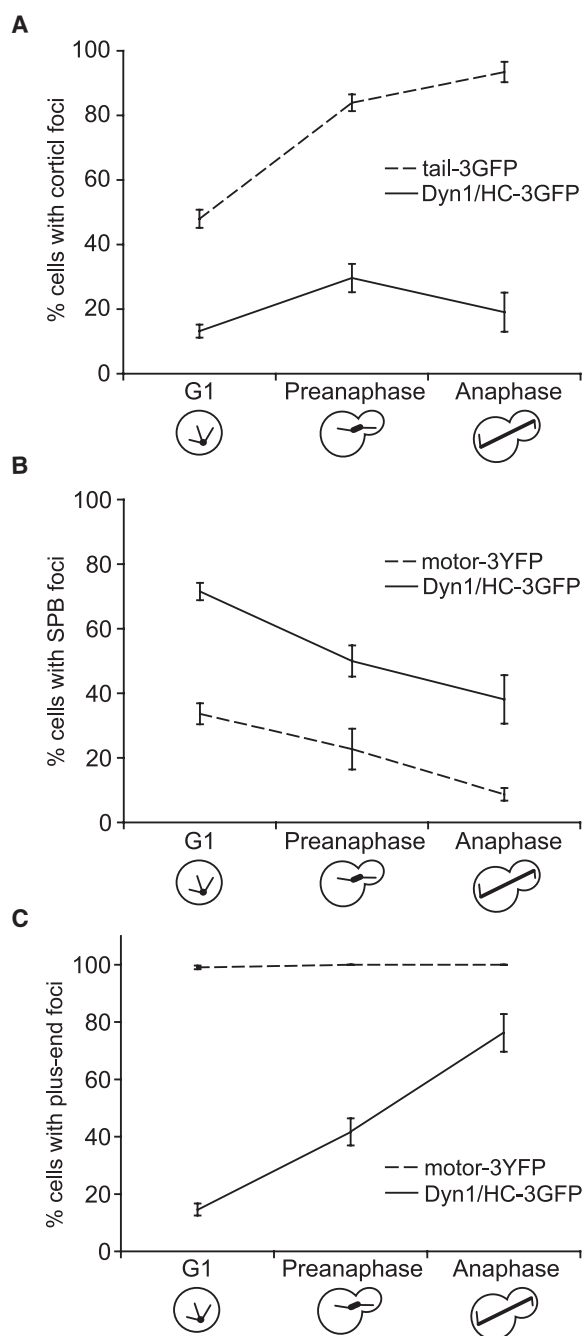


Figure 2. Cell-Cycle-Dependent Targeting of Dyn1/HC, Tail-3GFP, and Motor-3YFP

The percentage of cells in strains carrying *DYN1/HC-3GFP* ($n = 431$ cells), *TAIL-3GFP* ($n = 581$ cells), or *MOTOR-3YFP* ($n = 301$ cells) that display fluorescent foci at (A) the cell cortex, (B) the SPB, or (C) the plus end is plotted for the different cell-cycle stages. Each strain also expressed fluorescently labeled microtubules. A $2\text{ }\mu\text{m}$ Z-stack of images was collected at 5 s intervals for Dyn1/HC-3GFP, tail-3GFP, or motor-3YFP with mCherry-Tub1. Stationary cortical foci, SPB foci, and plus-end foci were identified in two-color movies and scored accordingly. Cells in G1, preanaphase, and anaphase were identified by brightfield and spindle morphology. Error bars represent standard error of proportion.

(Figure 3A; $80.3\% \pm 3.4\%$, $n = 137$). Furthermore, we detected fluorescence resonance energy transfer (FRET) from tail-3GFP to Num1-mCherry (Figure 3B, left). The mean calculated FRET_r

value was 2.4 ± 0.6 ($n = 13$) (Figure 3B, right), indicating specific FRET emission [25]. Therefore, our results showed that tail-3GFP and Num1-mCherry likely interact at the cell cortex.

We asked whether tail-3GFP colocalizes with Jnm1/p50, the yeast homolog of the dynactin subunit dynamitin, as would be expected if dynactin interacts with the dynein complex via association with the tail domain [26, 27]. We observed that the majority of tail-3GFP foci colocalized with Jnm1/p50-3mCherry foci (Figure 3C, top; $76.5\% \pm 3.0\%$, $n = 204$), indicating that the isolated tail domain assembles into a higher-order complex at the cell cortex. Together, these results demonstrate that tail-3GFP exhibits properties similar to Dyn1/HC-3GFP at the cell cortex.

Cortical Targeting of Tail-3GFP Is Independent of Plus-End Targeting

Next, we asked whether cortical tail-3GFP localization depends on components required for plus-end targeting of dynein, as would be expected if tail-3GFP is delivered to the cortex via the off-loading mechanism. The frequency of finding cortical tail-3GFP foci was unaffected in mutants lacking Pac1/LIS1, Bik1/CLIP-170, or Ndl1/NudEL (Figure 4A; Figure S1B), three components required for normal plus-end targeting of Dyn1/HC (Figure 4C) [22, 24, 28, 29]. Additionally, cortical tail-3GFP foci were absent in a *num1* Δ mutant (Figure 4A; Figure S1B), as previously reported for cortical Dyn1/HC-3GFP foci [17]. Immunoblot analysis revealed that tail-3GFP protein level was unaffected in *num1* Δ (Figure S1D). Thus, tail-3GFP is recruited to cortical Num1 directly from the cytoplasm, rather than being delivered by the microtubule plus end.

Furthermore, the frequency of finding cortical tail-3GFP foci was reduced in mutants lacking dynein accessory chains (Dyn3/LIC or Pac11/IC) or dynactin components (Arp1 or Nip100/p150) (Figure S2A). In *dyn3* Δ cells, tail-3GFP protein level was reduced, indicating a defect in protein stability (Figure S2C). However, the levels in *pac11* Δ , *arp1* Δ , and *nip100* Δ were similar to wild-type (Figure S2C; data not shown). Thus, assembly of tail-3GFP with other dynein and dynactin components may be required for stable association with cortical Num1, a result consistent with that of cortical Dyn1/HC-3GFP [17, 23].

In contrast to tail-3GFP, Dyn1/HC-3GFP depends on plus-end targeting components for localization to the cortex. In *pac1* Δ or *bik1* Δ mutants, in which plus-end targeting of Dyn1/HC-3GFP was reduced 8.9- and 5.7-fold (Figure 4C), respectively, we observed an 11.6- and 4.8-fold decrease in the frequency of finding cortical Dyn1/HC-3GFP foci, respectively, compared to wild-type cells (Figure 4C). Thus, cortical targeting of Dyn1/HC depends on plus-end targeting. Unlike tail-3GFP, direct recruitment of Dyn1/HC from the cytoplasm to Num1 does not occur. Our data suggest that the region in the tail domain responsible for interacting with Num1 is masked when Dyn1/HC cannot associate with microtubule plus ends.

The Motor Domain Targets Dynein to Spindle Pole Bodies and Plus Ends

The lack of SPB and plus-end localizations for tail-3GFP is in striking contrast to Dyn1/HC-3GFP. To test whether the motor domain is responsible for targeting dynein to these sites, we altered the *DYN1* locus to express only the motor domain (amino acids 1364–4092) [30] fused with 3YFP under its native promoter. In haploid cells carrying *MOTOR-3YFP* as their sole source of dynein, motor-3YFP localized to the SPB and plus ends (Figure 1C) and was notably absent from the cortex. Motor-3YFP

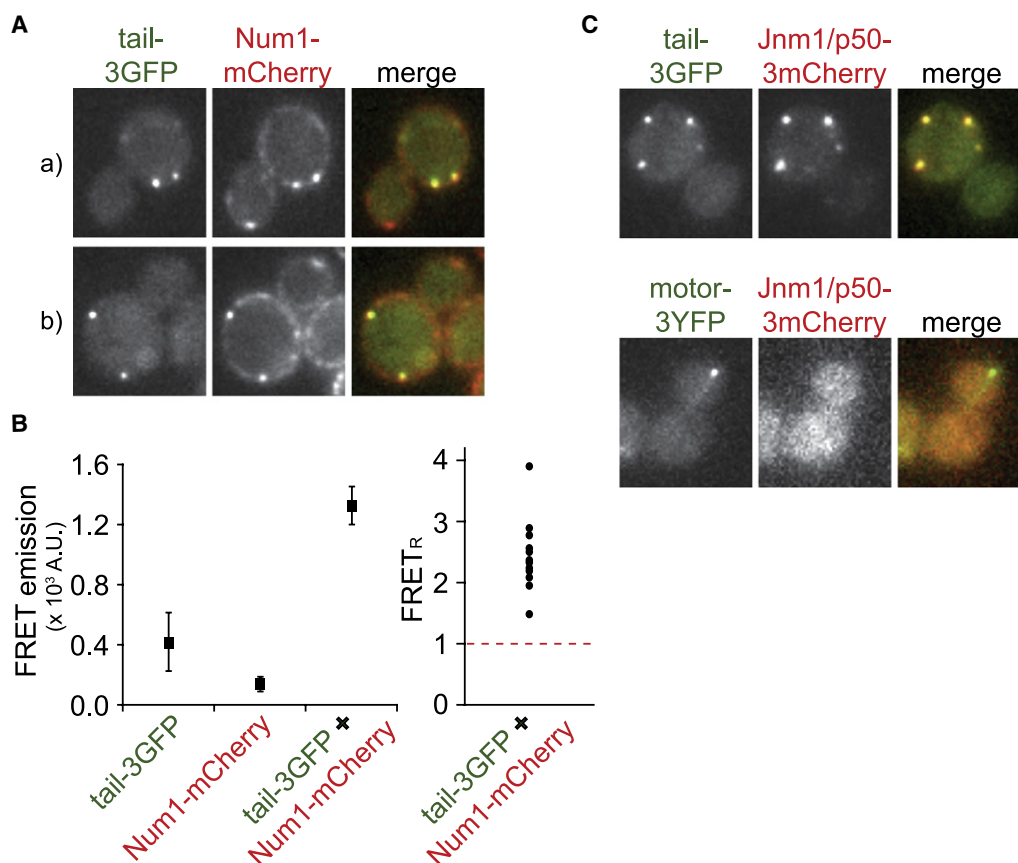


Figure 3. Tail-3GFP Associates with Num1-mCherry and Dynactin at the Cell Cortex

(A) Cells expressing tail-3GFP and Num1-mCherry (two examples are shown, indicated by a and b). Each image is a maximum intensity projection of a 3 μ m Z-stack of wide-field images. Merged image on the right depicts colocalization of the two tagged proteins, tail-3GFP in green and Num1-mCherry in red. (B) Left: Mean fluorescence intensity in the FRET channel (excitation $\lambda = 488$ nm; emission $\lambda > 560$ nm) was plotted for individual foci in strains expressing tail-3GFP only, Num1-mCherry only, or both. Right: Relative FRET values (FRET_R) for foci measured in *TAIL-3GFP NUM1-mCherry* strain ($n = 13$), calculated by dividing the background-corrected FRET channel fluorescence by the total spillover fluorescence, as described [25]. Tail-3GFP only and Num1-mCherry only strains were imaged to determine the spillover fluorescence into the FRET channel (see Supplemental Experimental Procedures). FRET_R values above 1, indicated by dashed red line, represent significant energy transfer above background. (C) Cells expressing dynactin subunit Jnm1/p50-3mCherry and tail-3GFP (top) or motor-3YFP (bottom). Each image is a maximum intensity projection of a 2 μ m Z-stack of wide-field images. Merged images on the right depict Jnm1/p50-3mCherry in red and tail-3GFP or motor-3YFP in green.

plus-end foci were dynamic (Figure 1D; Movie S4), associating with both growing and shrinking microtubules (Figure 1E; Movie S5). Additionally, motor-3YFP was often detected along the microtubule as speckles, which could be seen moving toward the plus end (Figure 1F; Movie S6), a behavior that was similarly observed for Dyn1/HC (see below; data not shown) [31]. These localization patterns demonstrate a novel role for the motor domain in SPB and plus-end targeting of dynein.

We compared the SPB and plus-end localizations of Dyn1/HC-3GFP and motor-3YFP. The frequency of finding Dyn1/HC-3GFP at the SPB decreased 1.9-fold from G1 to anaphase (Figure 2B). Motor-3YFP exhibited a similar pattern of decrease at the SPB (Figure 2B), although its frequency of targeting was always 2- to 4-fold lower than Dyn1/HC-3GFP. The frequency of finding Dyn1/HC-3GFP at the plus end was cell-cycle dependent, increasing 5.2-fold from G1 to anaphase (Figure 2C). Dyn1/HC-3GFP was largely absent from plus ends until preanaphase. In contrast, motor-3YFP was found at >99 % ($n = 301$) of plus ends irrespective of cell-cycle stage (Figure 2C). Thus, the tail domain, which is lacking from motor-3YFP, might play a role in regulating the cell-cycle-dependent accumulation of dynein at the plus end. As expected [23], plus-

end foci of motor-3YFP lacked dynactin complex, labeled with Jnm1/p50-3mCherry (Figure 3C, bottom). Thus, the tail domain of Dyn1/HC also recruits dynactin to the plus end.

Motor-3YFP Requires Pac1/LIS1 and Bik1/CLIP-170 for Accumulation at Plus Ends

We asked whether motor-3YFP targeting depends on its motor activity. Point mutations in the Walker A and Walker B motifs of the AAA3 unit, K2424A and E2488Q, respectively, block Dyn1/HC release from microtubules and inhibit dynein-mediated nuclear segregation [32, 33]. Neither mutation had any effect on motor-3YFP targeting (Figures S2D and S2E). Thus, motor activity is not required for plus-end targeting. Furthermore, the K2424A mutation did not affect full-length Dyn1/HC targeting to SPB, plus ends, and cortex (Figure S2F). Notably, plus-end foci containing Dyn1/HC_{K2424A}-3YFP often remained stably attached to a cortical spot for the entire duration of the movie (Movies S7 and S8). The Dyn1/HC_{K2424A}-3YFP found at the attachment sites may represent off-loaded and/or anchored dynein, which engaged with the plus end but failed in force production.

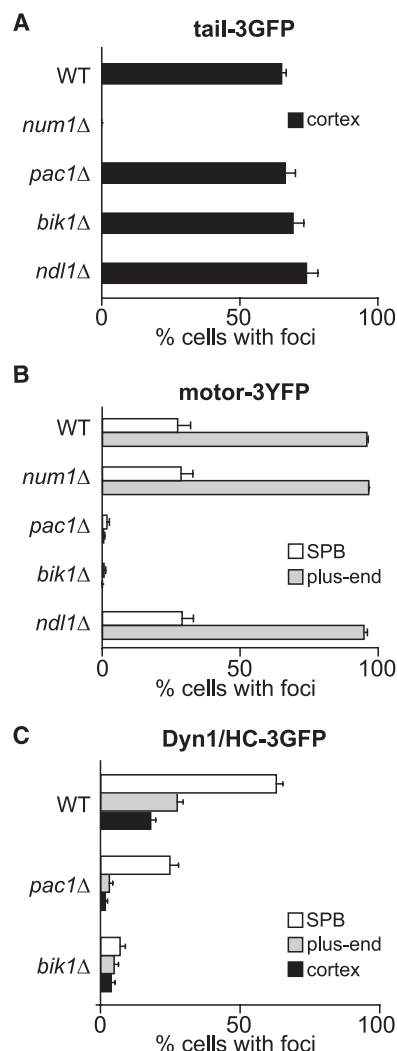


Figure 4. Localization of Tail-3GFP, Motor-3YFP, and Dyn1/Hc-3GFP in Null Mutants

The percentage of cells that display (A) tail-3GFP, (B) motor-3YFP, or (C) Dyn1/Hc-3GFP foci at a given subcellular site is plotted for different null mutants ($n > 100$ cells counted for each strain). To identify foci at the cortex, SPB, and plus end, a 2 μ m Z-stack of images was collected at 5 s intervals for each null strain expressing mCherry-Tub1 or CFP-Tub1 and either tail-3GFP, motor-3YFP, or Dyn1/Hc-3GFP. Movies were analyzed for foci at indicated locations. Error bars represent standard error of proportion.

We next asked whether motor-3YFP targeting depends on Pac1/LIS1, Bik1/CLIP-170, or Ndl1/NudEL. In *pac1Δ* and *bik1Δ* cells, the frequency of finding motor-3YFP foci at the SPB or plus ends was drastically reduced compared to wild-type cells (Figure 4B; Figure S1C). Immunoblot analysis of motor-3YFP revealed that protein levels were unchanged (Figure S1D). Thus, the dependence on Pac1/LIS1 and Bik1/CLIP-170 for plus-end targeting is similar to that of Dyn1/Hc-3GFP (Figure 4C) [22, 24]. In contrast, in *ndl1Δ* cells, no change in the frequency (Figure 4B; Figure S1C) or intensity (data not shown) of motor-3YFP targeting was observed. Thus, Ndl1/NudEL has no role in the plus-end localization of motor-3YFP, which is different from that of Dyn1/Hc-3GFP [29].

Furthermore, the frequency of finding motor-3YFP at the SPB or plus ends was unaffected in cells lacking dynein accessory components (Dyn3/LIC or Pac11/IC), dynactin

components (Arp1 or Nip100/p150), Num1, or Kip2 (a kinesin that transports Bik1/CLIP-170 to the plus end [28]) (Figure 4B; Figures S1C and S2B). To examine the role of Kip2, we combined *kip2Δ* with *kar3Δ*, so that microtubule length was normal [28]. In *kip2Δ kar3Δ* cells, although the frequency of targeting was unchanged, the intensities of the SPB foci increased (Figure S1E; 133.1% of wild-type) whereas those of the plus-end foci decreased (73.2% of wild-type). Additionally, we did not find speckles of motor-3YFP traveling along the length of microtubules in *kip2Δ kar3Δ* cells (Movie S9). Thus, taken together, the Kip2-dependent transport of speckles contributes to normal plus-end targeting of motor-3YFP.

Quantification of Dynein at Plus Ends

We used quantitative ratiometric methods to determine the number of fluorescent molecules at individual plus ends. Cse4, a stable kinetochore protein present at two copies per chromosome [34, 35], was used as a standard for the intensity measurements (Figure S3). On average, we found ~14, 13, and 5 copies of Dyn1/Hc-3mCherry per plus end, SPB, and cortical focus, respectively (Figure 5A; Figures S3D–3F). Because dynein is a dimer, these numbers represent ~7, 6.5, and 2.5 molecules of dynein complex, respectively. The intensities of motor-3YFP plus-end foci gave a broader distribution with a mean of ~45 copies per plus end (Figure 5B). Motor-3YFP is likely a monomer based on in vitro studies [30]. Thus, plus-end targeting of motor-3YFP is enhanced 6.3-fold compared to dimeric dynein molecules. In *num1Δ* cells, where Dyn1/Hc fails to off-load and is enhanced at the plus ends [22, 24], we found ~57 copies of Dyn1/Hc, or ~29 molecules of dynein complex, per plus end (Figure 5C). Thus, the observed level for motor-3YFP is similar to that for Dyn1/Hc in *num1Δ* ($p = 0.02$).

Motor-3YFP Blocks Plus-End Targeting and Function of Dyn1/Hc

We next asked whether the increased frequency and levels of motor-3YFP at plus ends would inhibit Dyn1/Hc function and localization, as predicted if motor-3YFP competes with Dyn1/Hc for plus-end targeting. We constructed a diploid strain carrying *MOTOR-3YFP* and *DYN1-2mCherry* at the two *DYN1* chromosomal loci, both under the control of the native promoter. The resulting diploid strain had a level of spindle misorientation similar to that of a dynein null strain, *dyn1Δ/3GFP* (Figure 6A), indicating a dominant-negative effect of *MOTOR-3YFP* on dynein pathway function [17, 22]. Strains carrying *MOTOR-3YFP* with the AAA3 point mutations (K2424A or E2488Q) also exhibited similar levels of spindle misorientation (Figure 6A). In contrast, strains carrying *TAIL-3GFP* or *3GFP* with *DYN1/Hc-2mCherry* did not exhibit any spindle misorientation defects (Figure 6A). Our findings are consistent with previous overexpression studies of dynein motor domain in *Dictyostelium* [36].

We further tested the effects of motor-3YFP on dynein pathway by assaying for synthetic growth defects with the Kar9 pathway. Budding yeast need either the dynein or Kar9 pathway for normal growth [17, 22]. Overexpression of motor-3YFP from a plasmid caused synthetic growth defects in *kar9Δ* and *bim1Δ*, two Kar9 pathway mutants, but not in *dyn1Δ* (Figure S4A). Overexpression of tail-3GFP or 3GFP did not cause synthetic growth defects (Figure S4A). Taken together, the spindle orientation and growth assays demonstrate that motor-3YFP, but not tail-3GFP, disrupt Dyn1/Hc function.

We next asked whether motor-3YFP blocked Dyn1/Hc function by inhibiting plus-end targeting of Dyn1/Hc. Motor-3YFP

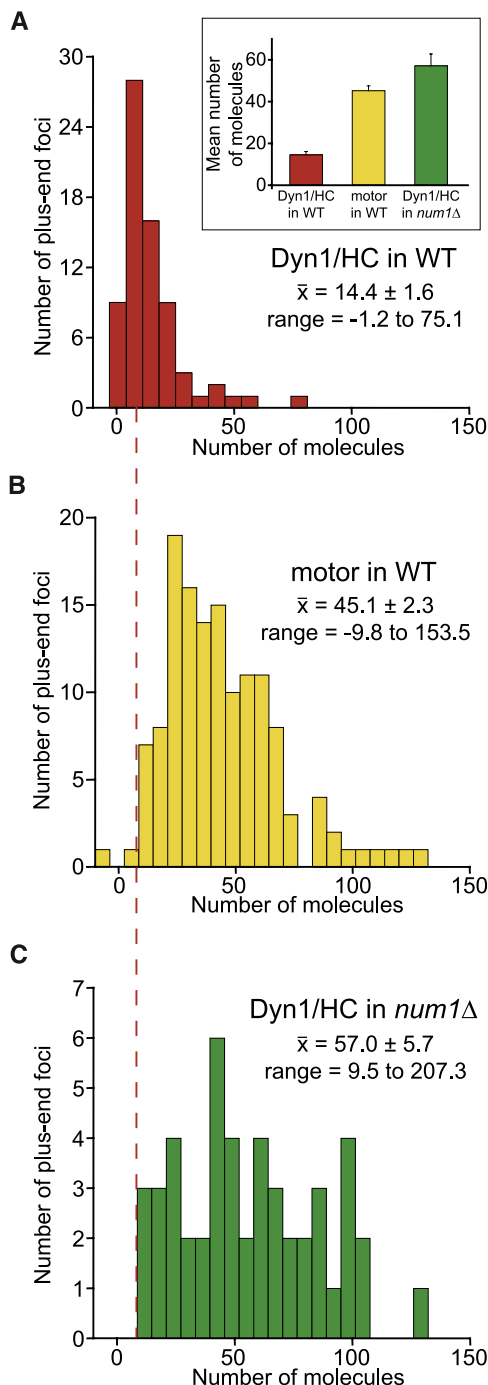


Figure 5. Quantitative Ratiometric Measurements of Plus-End-Associated Dyn1/HC and Isolated Motor Domain

(A) Histogram of the number of molecules of Dyn1/HC-3mCherry per plus-end focus in wild-type cells ($n = 71$). Fields containing a mixed population of strains expressing Cse4-3mCherry only or Dyn1/HC-3mCherry with CFP-Tub1 were imaged simultaneously to ensure identical imaging conditions. The mean fluorescence intensity of Cse4-3mCherry (Figure S3A) was assigned a value of 32 molecules of 3mCherry [34, 35] and was used to normalize Dyn1/HC-3mCherry fluorescence intensity (A.U.) to number of molecules. Inset graph depicts the mean number of molecules for (A), (B), and (C) with standard error. Vertical dashed red line indicates mean value for Dyn1/HC in wild-type cells.

(B) Histogram of the number of molecules of motor-3YFP per plus-end focus ($n = 137$). For normalizing motor-3YFP intensity, we used the intensity distribution of Dyn1/HC-3YFP as a standard (Figure S3B), which was normalized

(wild-type or AAA3 mutants), but not tail-3GFP, significantly reduced the frequencies of finding Dyn1/HC-3mCherry foci at plus ends and the cell cortex (Figure 6B). Loss of cortical Dyn1/HC-3mCherry caused by motor-3YFP further demonstrates that plus-end targeting of Dyn1/HC is a prerequisite for off-loading and anchoring at the cortex. We conclude that the dominant-negative capacity of motor-3YFP can be specifically attributed to its ability to block plus-end targeting of Dyn1/HC.

Overexpression of Pac1/LIS1 Rescues Motor-3YFP Dominant-Negative Effect at Plus Ends

Because Pac1/LIS1 and Bik1/CLIP-170 are required for plus-end targeting of motor-3YFP, it is possible that either one of them may be tightly sequestered by motor-3YFP, such that they are not free to recruit Dyn1/HC to plus ends. We asked whether we could relieve the dominant-negative effect of motor-3YFP by overexpressing Pac1/LIS1 or Bik1/CLIP-170. We used an inducible *GAL1* promoter to drive high expression of chromosomal *PAC1* or *BIK1* in the diploid strain carrying *MOTOR-3YFP* and *DYN1/HC-3mCherry*. Overexpression of Pac1/LIS1, but not Bik1/CLIP-170, rescued the dominant-negative effect of motor-3YFP on dynein pathway function, based on spindle misorientation assays (Figure 6C). Additionally, overexpression of Pac1/LIS1, but not Bik1/CLIP-170, restored targeting of Dyn1/HC-3mCherry to plus ends, SPB, and cell cortex to levels similar to those in a control strain without motor-3YFP (Figure 6D; Figure S4B). Movies of Pac1/LIS1-overexpressing cells showed speckles of Dyn1/HC-3mCherry moving along the cytoplasmic microtubules toward the plus end (Figure 6E; Movie S10). In contrast, overexpression of Bik1/CLIP-170 did not have an effect on Dyn1/HC-3mCherry targeting when motor-3YFP was present (Figure 6D; Figure S4B). We conclude that motor-3YFP inhibits dynein pathway function by sequestering Pac1/LIS1 from Dyn1/HC.

Discussion

In summary, we found that the tail domain targets Dyn1/HC to the cell cortex but not microtubule plus ends. We discovered that the motor domain is responsible for plus-end targeting of Dyn1/HC (Figure 7A). Our analysis reveals a new regulatory step that may involve an unmasking of the cortical association domain in Dyn1/HC (Figure 7B). Furthermore, we discovered that the isolated motor domain exhibits dominant-negative effects on Dyn1/HC targeting and function by tightly sequestering Pac1/LIS1.

The Role of Tail Domain in Dynein Function

We observed that tail-3GFP associates with the cortex more often than full-length Dyn1/HC. One possible explanation for this difference is that Dyn1/HC has an affinity for (and is sequestered by) microtubules (either along their length or at their plus ends) and SPBs. Thus, the concentration of free Dyn1/HC available to bind to the cortex is lower than that of tail-3GFP. Another possible explanation is that the cortical association domain is masked in the full-length Dyn1/HC molecule,

with the mean value of 14.4 copies of Dyn1/HC per plus end, as determined for Dyn1/HC-3mCherry in (A).

(C) Histogram of the number of molecules of Dyn1/HC-3GFP per plus end in *num1Δ* cells ($n = 52$). Cse4-3GFP (Figure S3C) was used as a standard, as in (A). Values less than zero are a result of background subtraction. Plus-end foci were identified with either CFP-Tub1 or mCherry-Tub1.

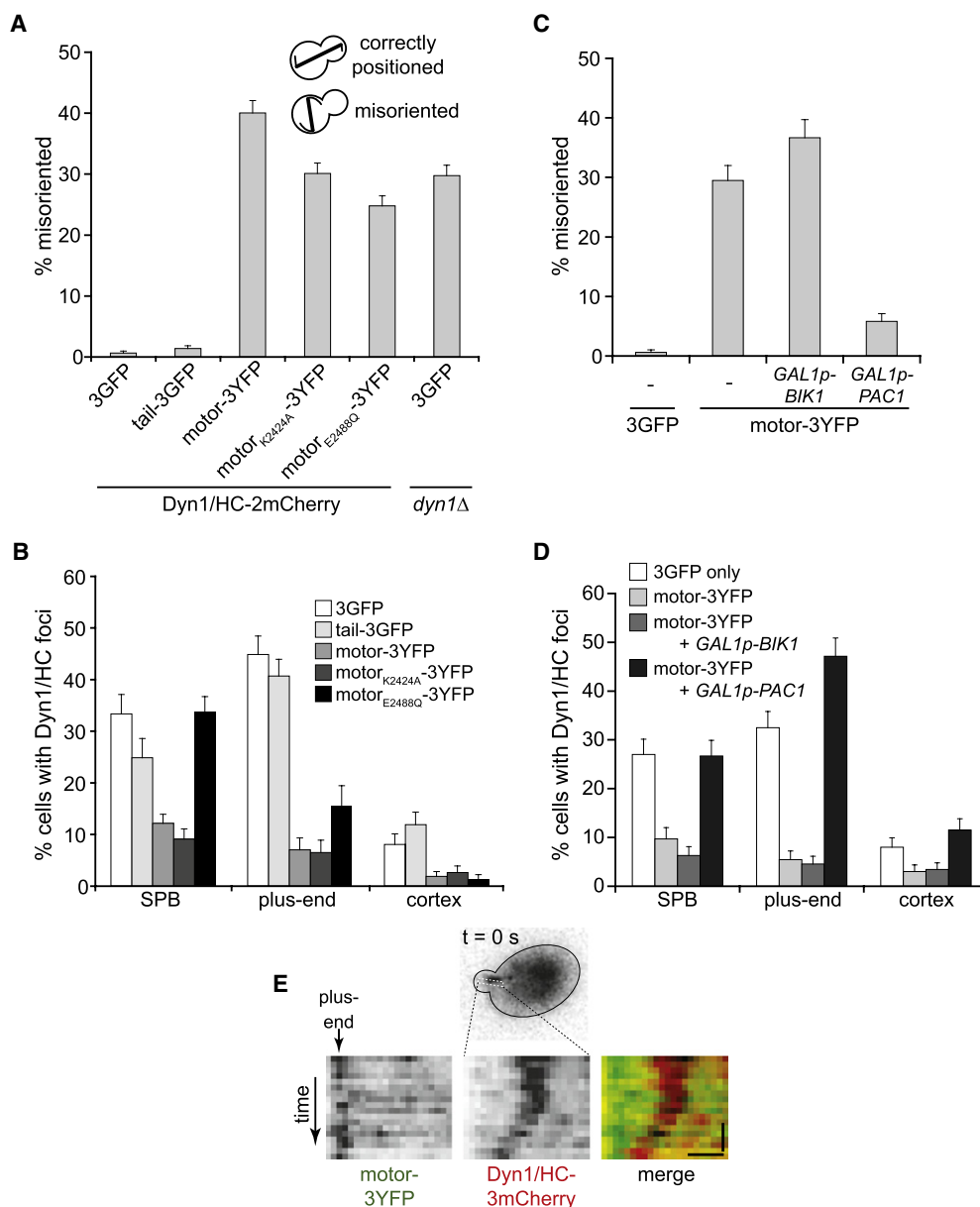


Figure 6. Dominant-Negative Effects of Motor-3YFP Can Be Rescued by Overexpression of Pac1/LIS1, but Not Bik1/CLIP-170

(A) The percentage of cells with a misoriented mitotic spindle in a cold (16°C) spindle position assay [24, 29] is plotted for diploid strains carrying *DYN1/HC-2mCherry* at one *DYN1* locus, and either 3GFP, TAIL-3GFP, or MOTOR-3YFP (wild-type or AAA3 mutants) at the other *DYN1* locus ($n > 570$ cells for each strain). The spindle was visualized with CFP-Tub1. A control diploid strain carrying no functional *DYN1* is indicated on the right.

(B) The percentage of cells that display Dyn1/HC-3mCherry foci at a given location is plotted for diploid strains similar to those in (A), except that the *DYN1/HC-2mCherry* allele was replaced with *DYN1/HC-3mCherry* for brighter fluorescence ($n > 150$ cells for each strain). Movies of Dyn1/HC-3mCherry and CFP-Tub1 were collected to distinguish foci at plus ends from SPB and the cell cortex. Strains were imaged after growth under the same conditions as in (A).

(C) The percentage of cells with a misoriented mitotic spindle in a cold spindle position assay is plotted for diploid strains carrying *DYN1/HC-3mCherry* and either 3GFP or MOTOR-3YFP, as indicated. The *GAL1* promoter was inserted at the 5' end of one of the chromosomal *BIK1* or *PAC1* loci. Strains were imaged after growth at 16°C to mid-log in synthetic defined media supplemented with 2% galactose ($n > 250$ cells for each strain).

(D) Percentage of cells that display Dyn1/HC-3mCherry foci at a given location is plotted for the same strains used in (C) and imaged after growth under the same conditions as in (C) ($n > 160$ cells for each strain).

(E) Kymograph depicting Dyn1/HC-3mCherry migrating along cytoplasmic microtubule toward a plus end in a Pac1/LIS1-overexpressing cell. The motor-3YFP signal was used as reference point to identify the plus end. Vertical bar represents 10 s; horizontal bar represents 1 μ m. See [Movie S10](#).

preventing it from binding to the cortex when it is free. Our findings did not support the former explanation, because free Dyn1/HC did not appear at the cortex when SPB and plus-end targeting were inhibited by deletion of Pac1/LIS1 or Bik1/CLIP-170 (Figure 4C) or when astral microtubules were

disrupted by nocodazole treatment (Figure S1F). Instead, cortical Dyn1/HC foci were reduced compared to wild-type. Given that Dyn1/HC protein has been shown to be stable in *bik1Δ* and *pac1Δ* cells [22, 24], we conclude that free Dyn1/HC fails to bind to the cortex in these cells because its

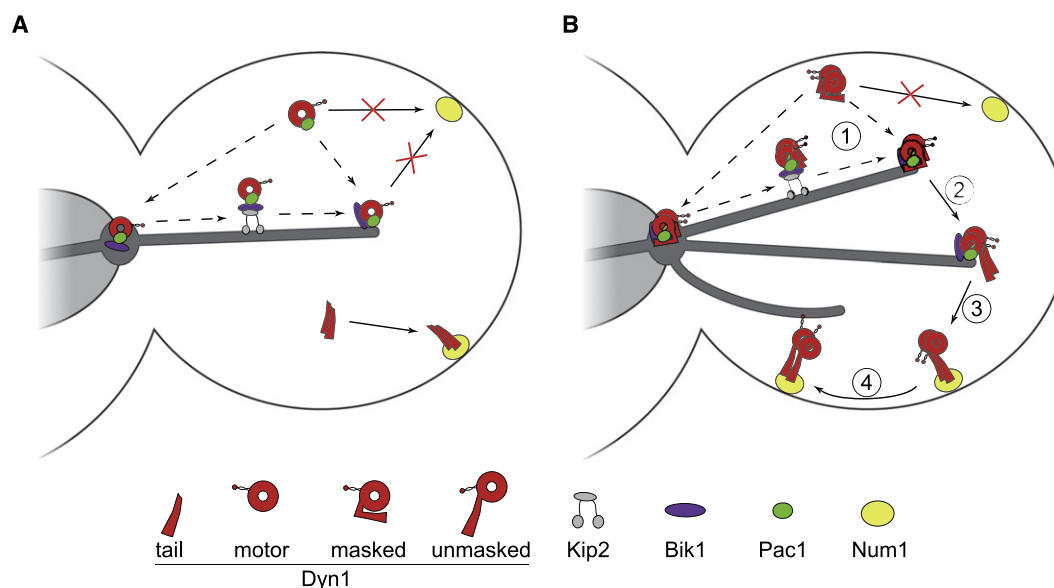


Figure 7. A Model for Dyn1/HC Unmasking at the Plus End

(A) Summary of results for *TAIL-3GFP* and *MOTOR-3YFP* strains. Isolated motor and tail domains are illustrated in the same cell.

(B) Prior to association with the cell cortex, our data indicate that the masked full-length Dyn1/HC molecule must first be targeted to microtubule plus ends (step 1). Our observations that Dyn1/HC and the isolated motor domain track along microtubules toward plus ends in a Kip2-dependent manner suggest that Dyn1/HC is actively transported in a manner similar to Bik1/CLIP-170 [28]. However, Dyn1/HC also appears to be recruited to plus ends directly from the cytoplasm. Upon association with plus ends, we propose that Dyn1/HC undergoes a conformational change (step 2), resulting in the unmasking of the N-terminal tail cortical association domain. Once unmasked, Dyn1/HC is primed for off-loading to the cell cortex (step 3), where it functions to power the sliding of astral microtubules (step 4). For simplicity, dynactin complex and dynein accessory chains were omitted in the illustration.

cortical-association domain is masked. The motor domain, or a motor domain-associated factor, likely performs this masking function.

Although targeting of tail-3GFP to the cell cortex is very robust, its presence does not interfere with the normal targeting and function of Dyn1/HC. This is not surprising given the large number of cortical Num1 foci (Figure 3A). This also indicates that receptor sites at the cell cortex are not limiting in the dynein pathway.

The Role of Motor Domain in Dynein Function

Molecule-counting measurements of Dyn1/HC and motor at the plus end reveal that, in a wild-type cell, Dyn1/HC is well below saturation. Our data indicate that there are approximately seven dynein complexes per microtubule plus end. Although this number is of similar magnitude to that previously reported for the dynactin complex at the plus end (mean ≈ 1 ; ≤ 5 dynactin complexes per plus end) [23], it is clear that Dyn1/HC is present at higher levels (Figure 5A; up to 38 dynein complexes per plus end). Thus, relative to dynein, dynactin at microtubule plus ends is limiting.

In contrast to tail, the motor inhibits dynein pathway activity by blocking Dyn1/HC targeting. The fact that Pac1/LIS1 overexpression is capable of rescuing this phenotype indicates that Dyn1/HC is unable to compete with the motor for Pac1/LIS1 binding. If the association between motor and Pac1/LIS1 was transient, upon their dissociation, Dyn1/HC and motor would have equal opportunity to compete for Pac1/LIS1 binding. Dyn1/HC would therefore be found at plus ends in equal proportion to motor; however, this was not observed (Figures 6B and 6D). Therefore, motor likely binds Pac1/LIS1 with much higher affinity than the full-length Dyn1/HC. This is consistent with *in vitro* studies by Reck-Peterson et al. [30],

who observed Pac1/LIS1 copurifying with the isolated motor but not the full-length molecule after microtubule affinity purification. The differential affinity of Pac1/LIS1 for the motor versus Dyn1/HC indicates that in the context of the full-length molecule, the tail domain plays a role in modulating Pac1/LIS1 binding to the motor domain. Previous studies in mammalian cells have demonstrated that LIS1 interacts with two distinct regions of the dynein heavy chain: one in the AAA1 unit of the motor domain and another in the tail domain [19]. Whether these interactions are conserved in yeast remains to be determined. The strong Pac1/LIS1 affinity state exhibited by the motor may represent a particular conformation adopted by Dyn1/HC throughout its life cycle; however, this phenomenon and the role of the tail domain in affecting this interaction requires further study.

In contrast to Dyn1/HC, motor does not require Ndl1/NudEL for plus-end targeting. Ndl1/NudEL has been proposed to affect plus-end targeting of Dyn1/HC by stabilizing the association between Dyn1/HC and Pac1/LIS1 [29]. The fact that Ndl1/NudEL is dispensable for plus-end targeting of motor is consistent with a stronger association of Pac1/LIS1 with the motor than with Dyn1/HC.

Although overexpression of Bik1/CLIP-170 did not rescue the dominant-negative effect of motor on dynein function, it altered the interaction of motor with astral microtubules. In Bik1/CLIP-170-overexpressing cells, the motor (likely in complex with Pac1/LIS1) decorated the entire length of astral microtubules and was less apparent as punctate foci (Figure S4B; compare control or *GAL1p-PAC1* to *GAL1p-BIK1*). Because Dyn1/HC targeting to microtubules was not rescued by Bik1/CLIP-170 overexpression (Figure 6D) and Pac1/LIS1 was limiting in the cell, we reason that binding of Dyn1/HC to Pac1/LIS1 represents a first step in the assembly

of a complex competent for plus-end targeting. Assembly of this complex with Bik1/CLIP-170 likely occurs subsequently.

Model for Dynein Unmasking at the Plus End

Previously, we proposed a model whereby dynein is off-loaded to the cell cortex from microtubule plus ends. Our data here support this model and reveal new insights into the mechanism underlying the spatial regulation of dynein. First, Dyn1/HC is targeted to plus ends by one of two mechanisms (Figure 7B, step 1, dashed lines): in a Bik1/CLIP-170- and Kip2-dependent manner, Dyn1/HC is transported along astral microtubules to the plus end; alternatively, Dyn1/HC is directly recruited to plus ends from the cytoplasm. This study and work from other labs [28, 29, 31] support both mechanisms of plus-end targeting. The former Kip2-dependent mechanism may account for ~30% of plus-end targeting (Figure S1E), and the latter accounts for ~70%. We propose that association of Dyn1/HC with the plus end triggers an unmasking of the tail domain (Figure 7B, step 2), which results in the consequent ability of Dyn1/HC to be off-loaded to Num1 sites at the cortex, its site of action (Figure 7B, step 3). Subsequently, cortically anchored dynein powers the sliding of astral microtubules (step 4), pulling the mitotic spindle toward the anchored site. Our analysis of full-length Dyn1/HC_{K2424A}-3YFP mutant (Figure S2F and Movies S7 and S8) demonstrates that cortically anchored Dyn1/HC is capable of capturing astral microtubule plus ends.

Dyn3/LIC and components of the dynactin complex have been implicated in the off-loading process, because their absence leads to the same phenotype as loss of Num1, namely loss of cortical Dyn1/HC foci and an enhancement of Dyn1/HC at the plus ends [17, 22, 23]. Because dynactin appears to be limiting at the plus-end relative to Dyn1/HC, association of dynactin with Dyn1/HC may be the crucial step in the regulation of the off-loading process, possibly through mediating the unmasking of the tail domain. This regulatory step may ensure that only fully assembled dynein-dynactin complexes are delivered to cortical sites.

Supplemental Data

Supplemental Data include Supplemental Experimental Procedures, four figures, one table, and ten movies and can be found with this article online at [http://www.current-biology.com/supplemental/S0960-9822\(09\)00540-5](http://www.current-biology.com/supplemental/S0960-9822(09)00540-5).

Acknowledgments

We thank Roy Kinoshita and Sean Christie for arranging Nikon microscope and cameras for use at MBL. We thank Dr. Moore and Dr. Schiebel for sending plasmids containing *MET3* promoter and *mCherry-TUB1*. We are grateful to Xianying Tang, Patricia Wadsworth, and Jennifer Ross for valuable discussions throughout this study. This work was supported by an HHMI Academic Research Internship and a University of Massachusetts Amherst Biology Department Junior Fellowship to J.J.P. and by an NIH/NIGMS grant (1R01GM076094) and a Laura and Arthur Colwin Endowed Summer Research Fellowship at MBL to W.-L.L.

Received: September 16, 2008

Revised: December 11, 2008

Accepted: December 15, 2008

Published online: January 29, 2009

References

- Gonczy, P., Pichler, S., Kirkham, M., and Hyman, A.A. (1999). Cytoplasmic dynein is required for distinct aspects of MTOC positioning, including centrosome separation, in the one cell stage *Caenorhabditis elegans* embryo. *J. Cell Biol.* 147, 135–150.
- Salina, D., Bodoor, K., Eckley, D.M., Schroer, T.A., Rattner, J.B., and Burke, B. (2002). Cytoplasmic dynein as a facilitator of nuclear envelope breakdown. *Cell* 108, 97–107.
- Schmidt, D.J., Rose, D.J., Saxton, W.M., and Strome, S. (2005). Functional analysis of cytoplasmic dynein heavy chain in *Caenorhabditis elegans* with fast-acting temperature-sensitive mutations. *Mol. Biol. Cell* 16, 1200–1212.
- Rusan, N.M., Tulu, U.S., Fagerstrom, C., and Wadsworth, P. (2002). Reorganization of the microtubule array in prophase/prometaphase requires cytoplasmic dynein-dependent microtubule transport. *J. Cell Biol.* 158, 997–1003.
- Goshima, G., Nedelec, F., and Vale, R.D. (2005). Mechanisms for focusing mitotic spindle poles by minus end-directed motor proteins. *J. Cell Biol.* 171, 229–240.
- Nguyen-Ngoc, T., Afshar, K., and Gonczy, P. (2007). Coupling of cortical dynein and G alpha proteins mediates spindle positioning in *Caenorhabditis elegans*. *Nat. Cell Biol.* 9, 1294–1302.
- O'Connell, C.B., and Wang, Y.L. (2000). Mammalian spindle orientation and position respond to changes in cell shape in a dynein-dependent fashion. *Mol. Biol. Cell* 11, 1765–1774.
- Howell, B.J., McEwen, B.F., Canman, J.C., Hoffman, D.B., Farrar, E.M., Rieder, C.L., and Salmon, E.D. (2001). Cytoplasmic dynein/dynactin drives kinetochore protein transport to the spindle poles and has a role in mitotic spindle checkpoint inactivation. *J. Cell Biol.* 155, 1159–1172.
- Wojcik, E., Basto, R., Serr, M., Scaerou, F., Kares, R., and Hays, T. (2001). Kinetochore dynein: its dynamics and role in the transport of the Rough deal checkpoint protein. *Nat. Cell Biol.* 3, 1001–1007.
- Koonce, M.P., and Sams, M. (2004). Of rings and levers: the dynein motor comes of age. *Trends Cell Biol.* 14, 612–619.
- Mocz, G., and Gibbons, I.R. (2001). Model for the motor component of dynein heavy chain based on homology to the AAA family of oligomeric ATPases. *Structure* 9, 93–103.
- Hook, P., and Vallee, R.B. (2006). The dynein family at a glance. *J. Cell Sci.* 119, 4369–4371.
- King, S.J., Bonilla, M., Rodgers, M.E., and Schroer, T.A. (2002). Subunit organization in cytoplasmic dynein subcomplexes. *Protein Sci.* 11, 1239–1250.
- King, S.M. (2000). The dynein microtubule motor. *Biochim. Biophys. Acta* 1496, 60–75.
- Vale, R.D. (2003). The molecular motor toolbox for intracellular transport. *Cell* 112, 467–480.
- Busson, S., Dujardin, D., Moreau, A., Dompierre, J., and De Mey, J.R. (1998). Dynein and dynactin are localized to astral microtubules and at cortical sites in mitotic epithelial cells. *Curr. Biol.* 8, 541–544.
- Lee, W.L., Kaiser, M.A., and Cooper, J.A. (2005). The offloading model for dynein function: differential function of motor subunits. *J. Cell Biol.* 168, 201–207.
- Purohit, A., Tynan, S.H., Vallee, R., and Doxsey, S.J. (1999). Direct interaction of pericentrin with cytoplasmic dynein light intermediate chain contributes to mitotic spindle organization. *J. Cell Biol.* 147, 481–492.
- Tai, C.Y., Dujardin, D.L., Faulkner, N.E., and Vallee, R.B. (2002). Role of dynein, dynactin, and CLIP-170 interactions in LIS1 kinetochore function. *J. Cell Biol.* 156, 959–968.
- Xiang, X., Han, G., Winkelmann, D.A., Zuo, W., and Morris, N.R. (2000). Dynamics of cytoplasmic dynein in living cells and the effect of a mutation in the dynactin complex actin-related protein Arp1. *Curr. Biol.* 10, 603–606.
- Grava, S., Schaerer, F., Faty, M., Philippsen, P., and Barral, Y. (2006). Asymmetric recruitment of dynein to spindle poles and microtubules promotes proper spindle orientation in yeast. *Dev. Cell* 10, 425–439.
- Lee, W.L., Oberle, J.R., and Cooper, J.A. (2003). The role of the lissencephaly protein Pac1 during nuclear migration in budding yeast. *J. Cell Biol.* 160, 355–364.
- Moore, J.K., Li, J., and Cooper, J.A. (2008). Dynactin function in mitotic spindle positioning. *Traffic* 9, 510–527.
- Sheeman, B., Carvalho, P., Sagot, I., Geiser, J., Kho, D., Hoyt, M.A., and Pellman, D. (2003). Determinants of *S. cerevisiae* dynein localization and activation: implications for the mechanism of spindle positioning. *Curr. Biol.* 13, 364–372.
- Muller, E.G., Snyderman, B.E., Novik, I., Hailey, D.W., Gestaut, D.R., Niemann, C.A., O'Toole, E.T., Giddings, T.H., Jr., Sundin, B.A., and Davis, T.N. (2005). The organization of the core proteins of the yeast spindle pole body. *Mol. Biol. Cell* 16, 3341–3352.

26. Tynan, S.H., Gee, M.A., and Vallee, R.B. (2000). Distinct but overlapping sites within the cytoplasmic dynein heavy chain for dimerization and for intermediate chain and light intermediate chain binding. *J. Biol. Chem.* 275, 32769–32774.
27. Vaughan, K.T., and Vallee, R.B. (1995). Cytoplasmic dynein binds dynactin through a direct interaction between the intermediate chains and p150Glued. *J. Cell Biol.* 131, 1507–1516.
28. Carvalho, P., Gupta, M.L., Jr., Hoyt, M.A., and Pellman, D. (2004). Cell cycle control of kinesin-mediated transport of Bik1 (CLIP-170) regulates microtubule stability and dynein activation. *Dev. Cell* 6, 815–829.
29. Li, J., Lee, W.L., and Cooper, J.A. (2005). NudEL targets dynein to microtubule ends through LIS1. *Nat. Cell Biol.* 7, 686–690.
30. Reck-Peterson, S.L., Yildiz, A., Carter, A.P., Gennerich, A., Zhang, N., and Vale, R.D. (2006). Single-molecule analysis of dynein processivity and stepping behavior. *Cell* 126, 335–348.
31. Caudron, F., Andrieux, A., Job, D., and Boscheron, C. (2008). A new role for kinesin-directed transport of Bik1p (CLIP-170) in *Saccharomyces cerevisiae*. *J. Cell Sci.* 121, 1506–1513.
32. Reck-Peterson, S.L., and Vale, R.D. (2004). Molecular dissection of the roles of nucleotide binding and hydrolysis in dynein's AAA domains in *Saccharomyces cerevisiae*. *Proc. Natl. Acad. Sci. USA* 101, 1491–1495.
33. Reck-Peterson, S.L., and Vale, R.D. (2004). Molecular dissection of the roles of nucleotide binding and hydrolysis in dynein's AAA domains in *Saccharomyces cerevisiae*. *Proc. Natl. Acad. Sci. USA* 101, 14305.
34. Meluh, P.B., Yang, P., Glowczewski, L., Koshland, D., and Smith, M.M. (1998). Cse4p is a component of the core centromere of *Saccharomyces cerevisiae*. *Cell* 94, 607–613.
35. Joglekar, A.P., Bouck, D.C., Molk, J.N., Bloom, K.S., and Salmon, E.D. (2006). Molecular architecture of a kinetochore-microtubule attachment site. *Nat. Cell Biol.* 8, 581–585.
36. Koonce, M.P., and Samso, M. (1996). Overexpression of cytoplasmic dynein's globular head causes a collapse of the interphase microtubule network in *Dictyostelium*. *Mol. Biol. Cell* 7, 935–948.